Universality in the fast orientational relaxation near isotropic–nematic transition

Article *in* The Journal of Chemical Physics · November 1998

DOI: 10.1063/1.477340

4 authors, including:

Sarangan Ravichandran
U.S. Department of Health and Human Services
98 PUBLICATIONS **2,111** CITATIONS

SEE PROFILE

Aurélien Perera
Sorbonne Université
119 PUBLICATIONS **2,558** CITATIONS

SEE PROFILE

Biman Bagchi
Indian Institute of Science
571 PUBLICATIONS **18,811** CITATIONS

SEE PROFILE

Universality in the fast orientational relaxation near isotropic–nematic transition

S. Ravichandran,[a] A. Perera, and M. Moreau
Laboratoire de Physique Théorique des Liquides, Université Pierre et Marie Curie, 75252 Paris Cedex 05, France

B. Bagchi[b]
Solid State and Structural Chemistry Unit, Indian Institute of Science, Bangalore 560 012, India

(Received 25 June 1998; accepted 31 July 1998)

Detailed molecular dynamics simulations of Lennard-Jones ellipsoids have been carried out to investigate the emergence of criticality in the single-particle orientational relaxation near the isotropic–nematic (IN) phase transition. The simulations show a sudden appearance of a power-law behavior in the decay of the second-rank orientational relaxation as the IN transition is approached. The simulated value of the power-law exponent is 0.56, which is larger than the mean-field value (0.5) but less than the observed value (0.63) and may be due to the finite size of the simulated system. The decay of the first-rank orientational time correlation function, on the other hand, is nearly exponential but its decay becomes very slow near the isotropic–nematic transition. The zero-frequency rotational friction, calculated from the simulated angular velocity correlation function, shows a marked increase near the IN transition. © *1998 American Institute of Physics*. [S0021-9606(98)52541-X]

I. INTRODUCTION

Orientational relaxation of elongated molecules near the isotropic–nematic (IN) phase transition has remained a subject of much discussion for the last three decades.[1–6] Usually the discussion is focused on the long-time dynamics where the relaxation is slow due to the emergence of the long-range orientational correlations near the IN transition. This long-time slow dynamics is known to exhibit several characteristics of critical dynamics.[3–6] The orientational anisotropy which can be measured by optical Kerr effect experiments is found to decay as a single exponential with a decay rate which slows down dramatically as the IN is approached.[7] This happens even though the IN transition is known to be weakly first order. The long-time dynamics has been rationalized in terms of Landau–de Gennes theory.[1,2] In typical experimental systems, this long-time dynamics set in after 1 ns. It seems that dynamics at shorter time scales were not considered in early investigations.

Recently, the existence of a new universal power-law dynamics for the orientational relaxation for the *initial part of the decay* near the IN has been proposed.[8] The experimental studies seem to suggest that the second-rank correlation function [which is the order parameter of the IN) decays, in the short time (1 ps to 1 ns range)] as

$$\langle Q(0)Q(t)\rangle \approx t^{-0.63}. \tag{1}$$

It is important to note that the measured single-particle rotational time constants in the liquid crystal forming liquids are in the picosecond range. Thus, this universal decay seems to appear immediately after the initial Gaussian decay (which always accompanies orientational relaxation as transients). Sengupta and Fayer presented an analysis of the origin of the universality in the fast relaxation. This analysis was based on a combination of ideas derived from mode coupling theory well known in critical dynamics and from the Landau–de Gennes theory. These authors showed that a straightforward application of the Landau–de Gennes theory would predict an exponent equal to 0.5 which is not surprising. As usual, the departure from this mean-field value of the exponent was attributed to the correction to the mean-field theory from short wavelength fluctuations.

While both the experimental evidence and the theoretical analysis of the existence of the universality are quite convincing, there remains several interesting questions to be answered on the orientational relaxation. First, what is the relation between the single particle and the collective orientational relaxation? This question has an important role to play in understanding the origin of the universality. Second, what happens to the first rank orientational correlation functions? In order to answer the above questions, we have carried out an extensive molecular dynamics (MD) simulation of Lennard-Jones ellipsoids.

The results of the computer simulations are rather startling. It is found that, near the IN transition, there is a sudden appearance of a temporal power law in the decay of the single-particle second-rank orientational time correlation function, which is in agreement with the experimental results and the theoretical analysis. The value of the exponent obtained in the simulations is equal to 0.56, which is intermediate between the mean-field prediction and the experimentally observed value. However, the main emphasis of this

[a]Present address: Department of Chemistry and Biochemistry, Duquesne University, Pittsburgh, PA.
[b]Also at the Jawaharlal Nehru Centre for Advanced Scientific Research, Bangalore, India.

work is on the observation and the analysis of the power-law decay of the dynamics.

Another important result of this work is the demonstration that the rotational friction itself should register a marked increase near the IN transition. This increase in the rotational friction and the accompanying decrease of the rotational diffusion constant are further signatures of the avoided criticality of the IN transition. Thus, in addition to the power-law behavior, the relaxation should also become stretched in time. This has also been observed in the simulations presented here. In many ways, the behavior of the orientational relaxation reminds one of the behavior observed in viscous liquids near its glass transition temperature.[9]

The organization of the rest of the paper is as follows. In Sec. II, we discuss the details of the system and the MD simulations. In Sec. III we present the results of the simulations. In Sec. IV we conclude with a brief discussion.

II. SYSTEM AND SIMULATION DETAILS

In this work we have used the Gay–Berne (GB) potential[10] to model the interaction between any two Lennard-Jones ellipsoids. Not only does it provide an analytic representation of interaction energy between two ellipsoids with arbitrary orientations, but it can also describe the isotropic–nematic (IN) transition successfully. The IN transition of ellipsoids GB potential have been studied extensively using MD simulations by De Miguel and co-workers.[11] They found a well-defined IN transition for aspect ratio $\kappa=3$ (where $\kappa=$ semi-major/semi-minor axis). These authors have studied in detail the static and dynamics of GB liquid near the isotropic–nematic (IN) transition. In an earlier work,[12] we reported MD results on orientation relaxation near the IN transition, but we did not search for the power-law temporal decay—our emphasis was on understanding the slow decay of the collective density fluctuations.

The ellipsoids are characterized by the aspect ratio κ which is the ratio of the length of the semi-major (a) to semi-minor (b) axes. The expression of the potential between a pair of molecules in the Gay–Berne model[10] is given by

$$U_{\mathrm{GB}}=4\epsilon(\hat{r},\hat{u}_1,\hat{u}_2)\left[\left[\frac{\sigma_0}{r-\sigma(\hat{r},\hat{u}_1,\hat{u}_2)+\sigma_0}\right]^{12}-\left[\frac{\sigma_0}{r-\sigma(\hat{r},\hat{u}_1,\hat{u}_2)+\sigma_0}\right]^{6}\right], \tag{2}$$

where $\hat{u}_1$ is the axial vector of molecule i, $\hat{r}$ is the unit vector along the intermolecular vector $\mathbf{r}=\mathbf{r}_2-\mathbf{r}_1$, where $\mathbf{r}_1$ and $\mathbf{r}_2$ denote the center of mass positions of molecules 1 and 2, respectively,[10] and $\sigma(\hat{r},\hat{u}_1,\hat{u}_2)$ and $\epsilon(\hat{r},\hat{u}_1,\hat{u}_2)$ are the orientation-dependent range and strength parameters, respectively.[10] In the above expression σ and ϵ depend on the aspect ratio κ (molecular elongation) and the anisotropy parameter κ' which is the ratio of the potential well depths of the side-by-side and end-to-end configurations.

A MD code has been developed for a system of 243 ellipsoidal particles interacting via the Gay–Berne potential.[10] The simulation box was cubic and the usual periodic boundary conditions were employed. The potential was cut and shifted at a distance of half-box length $[r_c^*=0.5(L/\sigma_0)]$. The translational and rotational equation motion was solved numerically using leap-frog method[13,14] considering a reduced moment of inertia of unity ($I^*=I/m\sigma_0^2$). The equation of motion was solved numerically with an integration time step of $\Delta t^*=\Delta t(m\sigma_0^2/\epsilon_0)^{-1/2}=0.0015$. In general the system was allowed to equilibrate over 50 000 time steps and averages were collected over 1×10^5 reduced time steps.

In this work we studied the GB fluid with aspect ratio $\kappa=3$ at temperature $T^*=kT/\epsilon_0=1.25$. For these values of the parameters, GB fluid undergoes a phase transition to nematic phase at $\rho^*=0.323$.

Near the IN transition, above the reduced density (ρ^*) 0.28, much longer runs have been performed to obtain reliable averages. Typically, trajectories were stored for 2×10^5 time steps and the averages were performed over this long trajectory.

In order to check the size dependence a single run was made at $\rho^*=0.3$ for 576 particles. The results obtained with 576 particles were similar to the 243 system reported in this study.

The dynamical behavior of the GB fluid has been analyzed in terms of the time correlation functions defined by

$$C_A(t)=\frac{\langle A(t_0)A(t_t)\rangle}{\langle A(t_0)A(t_0)\rangle}, \tag{3}$$

where $A(t)$ is a classical dynamical property of molecule i evaluated at time t. To study the reorientational motion, we have calculated the single-particle reorientational correlation functions defined by

$$C_{l0}^{(s)}(t)=\frac{\langle P_l[\hat{\mathbf{e}}_i(0)\cdot\hat{\mathbf{e}}_i(t)]\rangle}{\langle P_l[\hat{\mathbf{e}}_i(0)\cdot\hat{\mathbf{e}}_i(0)]\rangle}, \tag{4}$$

for $l=1$ and 2, where $\hat{\mathbf{e}}_i(t)$ is the unit vector along the symmetry axis of molecule i and P_l is the lth-order Legendre polynomial. In the above equations, the angular brackets imply an average over particles as well as over the time origins.

Results presented in this paper are all in the reduced units mentioned above which are standard for Gay–Berne potential.

III. RESULTS AND DISCUSSION

In Figs. 1–3 we show the density dependence of the reduced pressure, the isotropic pair distribution function, and the angular (220) component of the pair distribution function, respectively, up to a maximum density of $\rho^*=0.315$. As evident from these three figures, the simulated system remains on the isotropic branch for the densities studied here.

In Fig. 4, we present the log–log plot of the simulated single-particle second-rank ($l=2$) orientational time correlation function for eight densities starting from $\rho^*=0.1$ and ending at $\rho^*=0.315$. It is clear from the graph that the decay changes dramatically from a nearly exponential to a power-law behavior as density reaches to 0.315. Even at density 0.30, the decay is exponential. At $\rho^*=0.31$, one starts seeing the emergence of the power law behavior. For this system, the isotropic–nematic transition is known to be located at

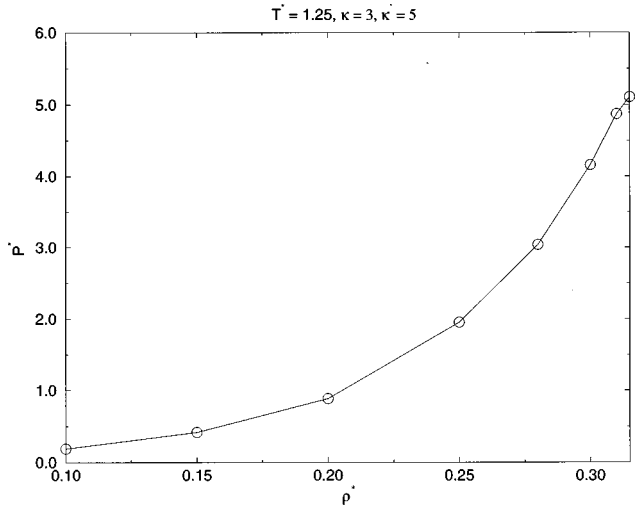

FIG. 1. The density dependence of pressure for a fluid of Gay–Berne liquid with aspect ratio equal to 3. Here the reduced density is $\rho^*=\rho\sigma_0^3$, where ρ is the number density and $P^*=P\sigma_0^3$. Here σ_0 is the length of the minor axis of the prolate ellipsoid.

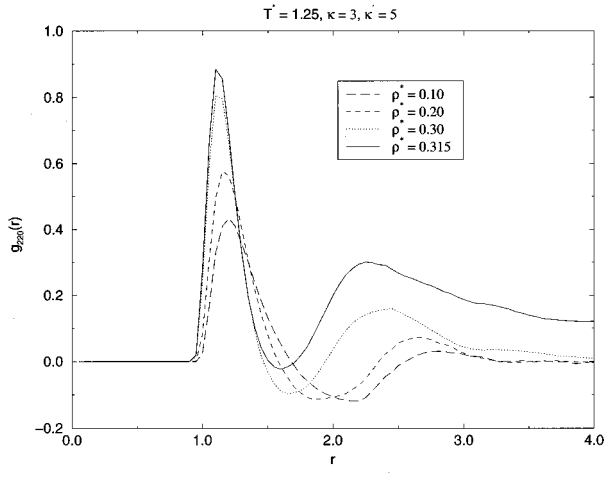

FIG. 3. The 220 component of the radial distribution function $g_{220}(r)$ is plotted for four reduced densities. The distribution at $\rho^*=0.315$ decays at longer distance.

$\rho^*=0.323$—a value confirmed in our simulations also. At density $\rho^*=0.315$, the value of the nematic order parameter is 0.32, which is typical in the transition region for the small system studied here. In Fig. 5 we show the log-log plot of the long-time decay of the simulated second-rank single-particle orientational correlation function along with the linear fit. We find here a slope of 0.56 (see Fig. 5).

Why does one observe a power-law decay even in a small system like the one simulated here? The reason can be understood by looking at the behavior of the collective orientational correlation function, $C_{20}(\mathbf{k},t)$,[15,16] defined by

$$C_{lm}(\mathbf{k},t)=\langle a_{lm}(\mathbf{k},t=0)a_{lm}(-\mathbf{k},t)\rangle, \tag{5}$$

where $a_{lm}(\mathbf{k},t)$ is defined by the following expression:

$$a_{lm}(\mathbf{k},t)=\int d\omega\ Y^*_{lm}(\omega)\,\delta\rho(\mathbf{k},\omega,t) \tag{6}$$

and

$$\delta\rho(\mathbf{k},\omega,t)=\sum_{l,m} a_{l,m}(\mathbf{k},t)Y_{l,m}(\omega). \tag{7}$$

In the above expressions $\mathbf{k}$ denotes the wave vector, ω represents the orientation of the molecule, and $Y_{lm}(\omega)$'s are the spherical harmonics of rank (l) and projection (m). This collective correlation function shows a marked slow down at small $\mathbf{k}$ which has already been captured in simulations.[12] This is due to the fact that the dynamical variable $a_{20}(\mathbf{k},t)$ (orientational order parameter) is not a conserved quantity.[15,16] Therefore, it can exhibit nearly critical dynamics even in a small system. The second important point is that $C^s_{20}(t)$ (Refs. 15 and 16), which is a single-particle quantity, is coupled to solvent dynamics at all wave vectors. When $C_{20}(\mathbf{k},t)$ undergoes a dramatic slow down near the IN transition, it affects the relaxation of the single-particle correlation function in a profound way, as found from the dra-

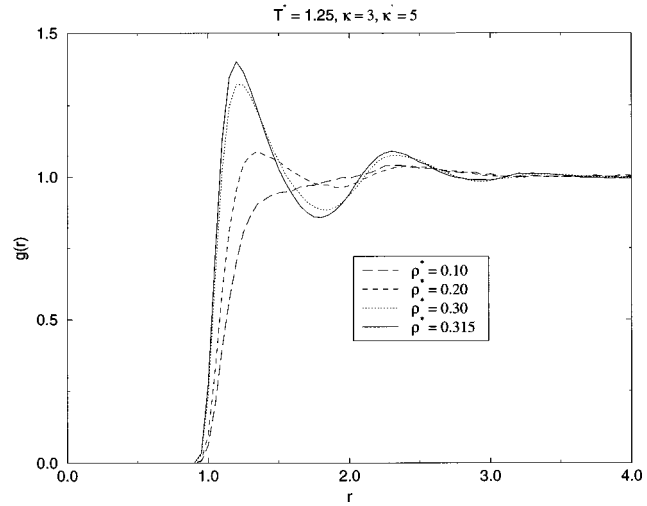

FIG. 2. Plot of the radial distribution function against distance r for different densities shown in the legand. Here the distance is scaled by σ_0.

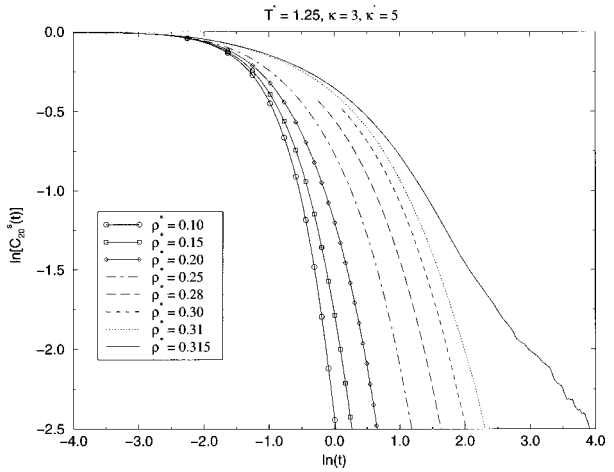

FIG. 4. The logarithm of the simulated single-particle second-rank orientational time correlation function, $C^s_{20}(t)$, is plotted against $\ln(t)$ for eight different reduced densities shown in the legend. As mentioned in the text, the averages for the three highest densities (0.3, 0.31, and 0.315) are performed over much longer runs.

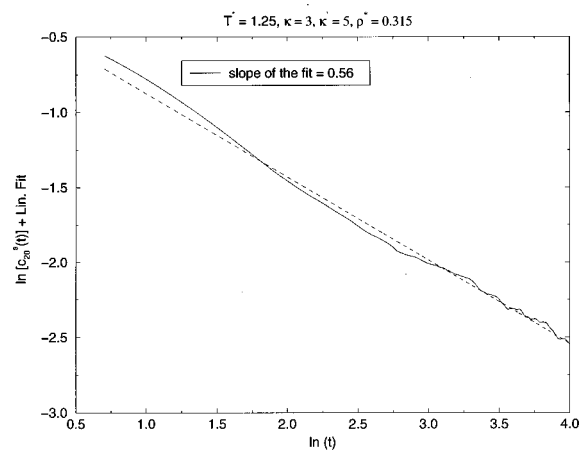

FIG. 5. The linear fit of the simulated second-rank orientational time correlation function against $\ln(t)$. The dashed fit gives the linear fit the data (solid line) with a slope of 0.56.

matic increase of the rotational friction. It should be noted that it is almost impossible to observe criticality due to *spatial* density fluctuations in a very small system.

In Fig. 6 we present the log–log plot of the simulated first-rank ($l=1$) single-particle orientational time correlation function, $C_{10}^s(t)$. Clearly, there is no power-law decay for $C_{10}^s(t)$ near the transition. However, the decay of the simulated $C_{10}^s(t)$ undergoes a pronounced slow down and becomes a nearly perfect exponential near the IN transition, as shown in Fig. 7. We regard this slow down of $C_{10}^s(t)$ interesting as it also arises from the slow down of the collective density fluctuations not directly but through the friction.[15]

In Fig. 8, we show the density dependence of the zero-frequency single-particle rotational friction $\zeta_R(z=0)$. The latter has been calculated from the following exact relation between $\zeta_R(z)$ and the simulated angular velocity correlation function $C_\omega(z)$:

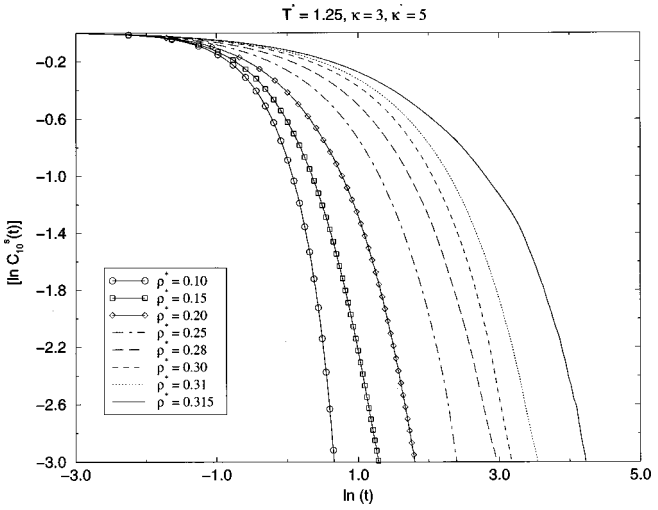

FIG. 6. The logarithm of the simulated single-particle first-rank orientational time correlation function, $C_{10}^s(t)$, is plotted against $\ln(t)$ for eight different reduced densities shown in the legend. As mentioned in the text, the averages for the three highest densities (0.3, 0.31, and 0.315) are performed over much longer runs.

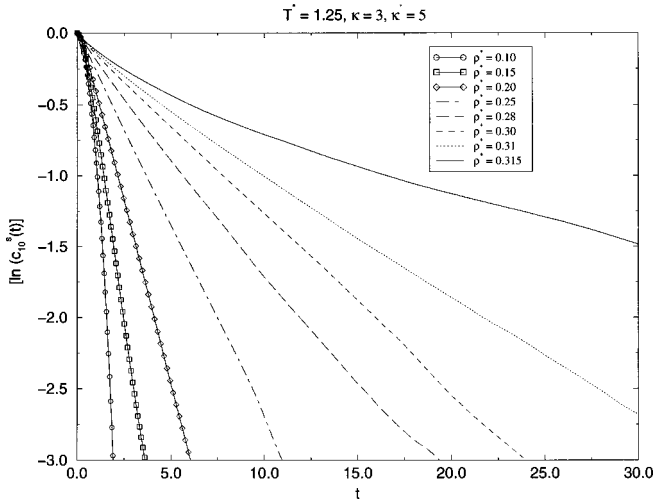

FIG. 7. The logarithm of the simulated single-particle first-rank orientational time correlation function, $C_{10}^s(t)$, is plotted against t for eight different reduced densities shown in the legend. As mentioned in the text, the averages for the three highest densities (0.3, 0.31, and 0.315) are performed over much longer runs.

$$C_\omega(z)=\frac{k_BT}{I[z+\zeta_R(z)]}, \tag{8}$$

where $C_\omega(z)$ and $\zeta_R(z)$ are the Laplace transformed forms of the respective time-dependent functions. Note that the rapid increase in the friction does not arise from any collisional Enskog type of friction, but rather from the coupling of the solute motion to collective density fluctuations which give rise to a slowly decaying force on the probe molecule.

There is a certain similarity between the power-law decay observed here and the power-law decays that are well known in the relaxation of glassy liquids.[9] In both the cases single-particle relaxation develops slow decay due to its coupling to the collective modes. In the case of supercooled liquid, the relaxation slows down due to the ''cage effect'' which is quantified by the first peak in the static structure factor which is also responsible for the slow down in the collective relaxation at the intermediate wave vectors. The

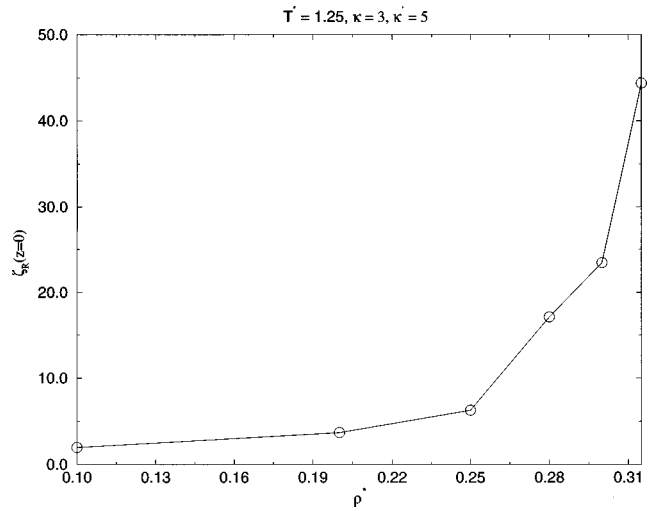

FIG. 8. The computed zero-frequency rotational friction $\zeta_R(z=0)$ is plotted against the reduced density. Note the rapid growth near the IN transition.

latter forces the slow down of the single-particle modes. In the present case of orientational relaxation near the IN transition, the slow down of the single-particle relaxation and the eventual power-law decay arises from the growth of correlations in the orientations. Here, however, the growth occurs at long wavelengths only. Thus, in the present case, the anomalous dynamics has a rather macroscopic (almost thermodynamic) origin while in glassy liquids the anomalous behavior has its origin in microscopic correlations.

IV. CONCLUSION

In this article we have presented molecular dynamics simulations in order to understand the observed power-law decay of the second-rank orientational correlation function. The simulations clearly show the emergence of the power-law decay of the orientational time correlation function *for the first time* in simulations for temperature-density conditions very close to the isotropic–nematic transition. The simulated value of power-law exponent is 0.56 which is larger than the mean-field prediction of 0.5 but less than the observed value of 0.63.[8] While the first rank orientational time correlation function shows exponential decay behavior as the IN transition is approached the decay slows down appreciably. This has been rationalized in terms of a dramatic increase in the single particle rotational friction. We have argued that the latter arises from the slow down in the collective orientational density fluctuations effect.

In the simulations, the appearance of the power law behavior is rather sudden. In experimental studies, however, this behavior seem to persist for a wide temperature range. This might be due to several reasons. First, the aspect ratio used in the simulation here is on the smaller side—the experimental aspect ratio is almost 5. Second, the system size is perhaps too small in simulations. One needs to be very close to the IN transition to find the growth in the correlation length necessary to produce the power law behavior.

The simulations here agree well with the experimental results.[8] The value of the exponent we find in simulation is 0.56, which is intermediate between the mean-field value of 0.5 and the experimental value of 0.63. This may again be due to the small size of the system studied. Nevertheless, the emergence of the power-law temporal decay behavior in simulations is rather remarkable. Further study of this problem is in progress.

ACKNOWLEDGMENTS

This work was supported by the Indo-French Center CEFIPRA under Project No. IFC/1106-1. Institut du Développement et des Ressources en Informatique Scientifique is thankfully acknowledged for the CPU time allocation on the CRAY C98. We also wish to thank Centre de Calcul et de Recherches of Jussieu for generous allocation of computation time.

[1] P. G. de Gennes, *The Physics of Liquid Crystals* (Clarendon, Oxford, 1974).
[2] S. Chandrasekhar, *Liquid Crystal*, 2nd ed. (Cambridge, New York, 1992).
[3] B. Chu, C. S. Bak, and F. L. Lin, Phys. Rev. Lett. **28**, 1111 (1972).
[4] E. Gulari and B. Chu, J. Chem. Phys. **62**, 798 (1975).
[5] C. Flytzanis and Y. R. Shen, Phys. Rev. Lett. **33**, 14 (1974).
[6] F. W. Deeg, S. R. Greenfield, J. J. Stankus, V. J. Newell, and M. D. Fayer, J. Chem. Phys. **93**, 3503 (1990).
[7] J. J. Stankus, R. Torre, and M. D. Fayer, J. Phys. Chem. **97**, 9478 (1993).
[8] A. Sengupta and M. D. Fayer, J. Chem. Phys. **102**, 4193 (1995).
[9] M. Ediger, C. A. Angell, and S. Nagel, J. Phys. Chem. **100**, 13 200 (1996); M. T. Cicerone and M. D. Ediger, J. Chem. Phys. **103**, 5684 (1995).
[10] J. G. Gay and B. J. Berne, J. Chem. Phys. **74**, 3316 (1981).
[11] E. De Miguel, L. F. Rull, M. K. Chalam, K. E. Gubbins, and F. Van Swol, Mol. Phys. **72**, 593 (1991).
[12] A. Perera, S. Ravichandran, M. Moreau, and B. Bagchi, J. Chem. Phys. **106**, 1280 (1997).
[13] M. P. Allen and D. J. Tildesley, *Computer Simulation of Liquids* (Clarendon, Oxford, 1987).
[14] D. Fincham, Daresbury Laboratory Information Quarterly for MD and MC Simulations (CCP5 Quarterly) **12**, 47 (1984).
[15] B. Bagchi and A. Chandra, Adv. Chem. Phys. **80**, 1 (1991) (and references therein); S. Ravichandran and B. Bagchi, Int. Rev. Phys. Chem. **14**, 271 (1995); A. Chandra and B. Bagchi, J. Chem. Phys. **91**, 1829 (1989).
[16] A. Chandra and B. Bagchi, Physica A **169**, 246 (1990).